

AC  
BIBLIOTHEQUE

TRI-pp-85-108  
Dec 1985

11 SEP. 1986

TWO-PHOTON DECAY WIDTHS OF HIGGS BOSONS  
IN MINIMAL BROKEN SUPERSYMMETRY

R. Bates and John N. Ng

Theory Group, TRIUMF  
4004 Wesbrook Mall, Vancouver, B.C., Canada V6T 2A3

and  
P. Kalyniak

Physics Dept., Carleton University  
Ottawa, Canada K1S 5B6

Abstract

The two photon decay widths of non-standard Higgs bosons are studied in a minimal broken supersymmetry model. For two Higgs doublet models in general, a large enhancement of these widths relative to the standard model is possible. However, we find for the case studied that a severe upper bound on this possible enhancement is imposed by the supersymmetry features of the model. With only the t-quark as the heaviest fermion we find a two-photon width of 100 keV for a 160 GeV/c<sup>2</sup> scalar Higgs boson is possible. The corresponding width for a pseudoscalar is 60 keV.

CERN LIBRARIES, GENEVA



CM-P00067472

In a previous paper [1] we studied the two photon decays of spin-0 Higgs mesons in a supersymmetric standard model with SU(2)xU(1) gauge symmetry. Hereafter this model is referred to as SSSM. It was found that unlike the g-2 of the leptons, the two-photon widths of both scalar and pseudoscalar Higgs bosons do not vanish in the supersymmetric limit. In the SSSM the gauge symmetry is broken by a SU(2) and U(1) singlet Higgs field, N. Being supersymmetric the SSSM is not realistic. In this paper we study the decay widths of neutral scalars and pseudoscalars, collectively denoted by X<sup>0</sup>, into two photons in a SSSM with broken supersymmetry. Our motivation is phenomenological. If the mass of X<sup>0</sup> is such that it can be produced at SLC or LEP via reactions such as

$$e^+e^- + Z^0X^0$$
$$e^+e^- + \mu^+\mu^-X^0$$

and/or

the two-photon decay mode of X<sup>0</sup> will certainly be a spectacular one to detect. This will even be more important if this width can be enhanced in realistic broken supersymmetric gauge theory when compared to the standard model Higgs boson, H<sup>0</sup>. An enhanced two-photon width can lead to enhanced production of these bosons via the two-photon mechanism in e<sup>+</sup>e<sup>-</sup> annihilation [2]. In the standard model with 3 families of quarks and leptons, the two-photon width,  $\Gamma_{\gamma\gamma}$ , of a H<sup>0</sup> of mass M<sub>H</sub> was calculated [2,3] to be

$$\Gamma_{\gamma\gamma} = \frac{\alpha^3 M_H^3 |A|^2}{16\pi^2 \sin^2\theta_w M_w^2} \quad (1)$$

The quantity |A|<sup>2</sup> is a dimensionless function with weak dependence on the ratios M<sub>w</sub><sup>2</sup>/M<sub>H</sub><sup>2</sup> and m<sub>L</sub><sup>2</sup>/M<sub>H</sub><sup>2</sup> where M<sub>w</sub> and m<sub>L</sub> are the masses of the W-boson and

the t-quark respectively. For a large range of  $M_H$ , say between 40 to 160 GeV/c<sup>2</sup> we can approximate eq. (1) by

$$\Gamma_{\gamma\gamma} \approx 10^{-5} M_H^3 \text{ keV} \quad (1')$$

with  $M_H$  measured in units of GeV/c<sup>2</sup>. Hence, even for a 100 GeV/c<sup>2</sup>  $H^0$ , the two-photon width is only about 10 keV.

The purpose of this paper is to study the effect of introducing supersymmetry into the picture. To be specific we employ a minimal SSSM where the gauge symmetry is broken by a SU(2) and U(1) singlet Higgs field and the supersymmetry breaking is achieved via soft breaking terms induced by supergravity at the scale of the Planck mass,  $M_p$ . Passage from N=1 supergravity to the effective low energy Lagrangian is depicted by [4]

$$\mathcal{L}_{(N=1 \text{ supergravity})} \xrightarrow{M_p} \mathcal{L}_{\text{SSSM}} + \mathcal{L}_{\text{SSB}}$$

where  $\mathcal{L}_{\text{SSB}}$  denotes the supersymmetry breaking Lagrangian. The general structure of  $\mathcal{L}_{\text{SSB}}$  is given in ref. [5]. Details of the specific model will be spelled out in sec. 2. At the tree level, we find that the charged Higgs masses give non-trivial constraints on the parameters of the effective Lagrangian. This appears not to have been discussed before.

In sec. 3 we give details of the calculation of  $\Gamma_{\gamma\gamma}$  within this low energy broken supersymmetry model. Section 4 compares the width with that of the standard  $H^0$  and discusses the phenomenological importance of these decays. Technical details of the Feynman diagrams are given in the appendix A where a complete list of the vertices necessary for calculating  $\Gamma_{\gamma\gamma}$  is also presented.

## 2. Minimal broken supersymmetric standard model

The total interaction Lagrangian,  $\mathcal{L}_{\text{int}}$ , is divided into a supersymmetric piece,  $\mathcal{L}_{\text{SS}}$ , and a piece which softly breaks supersymmetry,  $\mathcal{L}_{\text{SSB}}$ . Thus, we have

$$\mathcal{L}_{\text{int}} = \mathcal{L}_{\text{SS}} + \mathcal{L}_{\text{SSB}} \quad (2.1)$$

The supersymmetric part,  $\mathcal{L}_{\text{SS}}$  is constructed out of the fields listed in table 1. Three sets of Higgs field,  $H_1, H_2$  and  $N$  are employed to break the SU(2) $\times$ U(1) symmetry [6]. We shall be interested only in one quark lepton family and thus the quark mixings and family labels will be omitted. These can be included straightforwardly. A derivation of  $\mathcal{L}_{\text{SS}}$  from superfield formalism can be obtained in ref. [1].

For clarity and completeness we will present  $\mathcal{L}_{\text{SS}}$  in several pieces. The interactions of the gauge multiplets among themselves and the matter fields are described by  $\mathcal{L}_{\text{gauge}}$ . This is given by

$$\begin{aligned} \mathcal{L}_{\text{gauge}} = & ig\sqrt{2} T_{ij}^a (\lambda^a \psi_{iA}^* - \bar{\lambda}^a \bar{\psi}_{iA}) + \frac{ig'}{\sqrt{2}} (\lambda^1 \psi_{iA}^* - \bar{\lambda}^1 \bar{\psi}_{iA}) \\ & - ig T_{ij}^a v_\mu^a \{ [A_i^* \partial^\mu A_j - (\partial^\mu A_i^*) A_j] - i \bar{\psi}_i \sigma^\mu \psi_j \} \\ & - \frac{ig'}{2} v'_\mu \{ y_A [A^* \partial^\mu A - (\partial^\mu A) A] - i y_f \bar{\psi} \sigma^\mu \psi \} \\ & + A_i^* A_j (g T_{ik}^a v_\mu^a + \frac{1}{2} g' y_A \delta_{ik} v'_\mu) (g T_{kj}^b v^{\mu b} + \frac{1}{2} g' y_A \delta_{kj} v'^{\mu}) \\ & + ig \epsilon_{abc} \bar{\lambda}^a \sigma^{\mu\lambda} b_\nu \gamma_\mu^c \end{aligned} \quad (2.2)$$

In the above equation, we have used  $A$  to denote the scalar fields and  $\psi$  represents generically the Majorana matter spinor fields of table 1. The U(1) hypercharge of the scalar field  $A$  is  $y_A$  and that of the matter fermion field is  $y_f$  and  $\sigma^\mu = (1, \vec{\sigma})$  where  $\vec{\sigma}$  denotes the three Pauli matrices. A sum over all scalar fields  $A$  is implicit. The SU(2) generators are  $T_{ij}^a$  where  $a=1,2,3$  and  $i,j=1,2$ .

A second piece,  $\mathcal{L}_Y$ , describes the Yukawa interactions between the fermions and the scalar bosons. We include here also the scalar-fermion Higgs field interactions since they are the supersymmetric partner interactions to the Yukawa ones. Explicitly, we have

$$\begin{aligned} \mathcal{L}_Y = & \epsilon_{1j} f_e H_1^j \bar{L}^j e_R + h.c. + f_d^2 |H_1^j|^2 e_R^{*k} + |f_e \epsilon_{1j} \bar{L}^j e_R + h_d \epsilon_{1j} \tilde{Q}^j d_R|^2 + |h_u \epsilon_{1j} \tilde{Q}^j u_R|^2 \\ & + 2\text{Re} [h_e \epsilon_{1j} H_1^j \tilde{L}^j (f_e \epsilon_{1k} \tilde{L}^k e_R + h_d \epsilon_{1k} \tilde{Q}^k d_R)^*] + 2\text{Re} [(h_e \epsilon_{1j} H_1^j N)(h_u \epsilon_{1k} \tilde{Q}^k u_R)^*] \\ & + |f_e \epsilon_{1j} H_1^j \tilde{L}^j|^2 + \epsilon_{1j} h_d H_1^j \tilde{Q}^j d_R + h.c. + |h_d \epsilon_{1j} H_1^j \tilde{Q}^j|^2 + |h_u \epsilon_{1j} H_1^j \tilde{Q}^j|^2 \\ & + \epsilon_{1j} h_u H_1^j \tilde{Q}^j u_R + h.c. + |(h_d H_1^j \tilde{d}_R - h_u H_1^j \tilde{u}_R)|^2 \end{aligned} \quad (2.3)$$

where  $f_e$ ,  $h_d$  and  $h_u$  are the Yukawa couplings. As usual  $\mathcal{L}_Y$  gives rise to quark (squark) and lepton (slepton) masses. In the absence of the supersymmetry breaking term the fermion and corresponding sfermions will have degenerate masses. The third piece,  $\mathcal{L}_S$ , is the superpotential. It is given by [7],

$$\begin{aligned} -\mathcal{L}_S = & V \\ = & h^2 (|H_1^j|^2 + |H_2^j|^2) |N|^2 + |h_e \epsilon_{1j} H_1^j H_2^j + s|^2 \\ & + \frac{1}{8} g^2 \{4 |H_1^j H_2^j|^2 - 2 |H_1^j|^2 |H_2^j|^2 + \sum_{m=1,2} [4 |H_m^j \tilde{Q}_L^j|^2 - 2 |H_m^j|^2 |\tilde{Q}_L^j|^2 \\ & + 4 |H_m^j \tilde{L}_L^j|^2 - 2 |H_m^j|^2 |\tilde{L}_L^j|^2] + 4 |\tilde{Q}_L^j|^2 |\tilde{L}_L^j|^2 - 2 |\tilde{Q}_L^j|^2 |\tilde{L}_L^j|^2 \\ & + |H_1^j|^4 + |H_2^j|^4 + |\tilde{Q}_L^j|^4 + |\tilde{L}_L^j|^4\} \\ & + \frac{1}{8} g'^2 \{ |H_1^j|^2 - |H_2^j|^2 + \frac{1}{3} |\tilde{Q}_L^j|^2 - \frac{4}{3} |\tilde{U}^j|^2 + \frac{2}{3} |\tilde{D}^j|^2 + 2 |\tilde{e}_R^j|^2 \}^2 \end{aligned} \quad (2.4)$$

where  $|A^j|^4 \equiv (A^{j*} A^j)^2$  for the scalar field A. Finally the usual gauge-fixing Lagrangian  $\mathcal{L}_{GF}$  and the Faddeev-Popov ghost Lagrangian  $\mathcal{L}_{FP}$  have

to be added. We work in the 't Hooft-Feynman gauge. Adding them together the supersymmetric standard model Lagrangian is just

$$\mathcal{L}_{SS} = \mathcal{L}_{\text{gauge}} + \mathcal{L}_Y + \mathcal{L}_S + \mathcal{L}_{GF} + \mathcal{L}_{FP} \quad (2.5)$$

The above interaction Lagrangian is globally supersymmetric. To be phenomenologically realistic supersymmetry must be broken. This can be achieved by soft breaking terms [5] which presumably arise from supergravity. The effective low energy, i.e. below the Planck mass, Lagrangian that breaks supersymmetry can be written as [8,9]

$$\begin{aligned} \mathcal{L}_{SSB} = & -\frac{1}{2} \tilde{m}^2 (\lambda^j \lambda^j + \bar{\lambda}^j \bar{\lambda}^j) - \frac{1}{2} \tilde{m} (\lambda^j \lambda^j a + \bar{\lambda}^j \bar{\lambda}^j a) \\ & - \sum_A m_A^2 A^* A - m_{3/2} (h(Z) + h.c.) \end{aligned} \quad (2.6)$$

where  $h(Z) = (A-3)g(Z) + \sum_A \frac{\partial g}{\partial Z_A} Z_A$  (2.7a)

$$\begin{aligned} g = & (h_e \epsilon_{1j} H_1^j H_2^j N + sN) \\ & + f_e \epsilon_{1j} H_1^j \tilde{L}^j e_R + h_d \epsilon_{1j} H_1^j \tilde{Q}^j d_R \\ & + h_u \epsilon_{1j} H_1^j \tilde{Q}^j u_R + h.c. \end{aligned} \quad (2.7b)$$

As before sum over A represents a sum over all the scalar fields. The gaugino masses  $\tilde{m}^j$  and  $\tilde{m}$  as well as the gravitino mass  $m_{3/2}$  are free parameters. Eq. (2.7a) contains terms that split the degeneracy in the masses of the sfermions and fermions. Because of simplicity and the added attraction of having a structure close to the supersymmetric model, we take the parameter A, governing the Goldstino-matter coupling in eq. (2.7a) to be [8] A=3.

It is often argued that the gaugino and the scalar masses can be taken to be all equal to the  $m_{3/2}$  at the Planck scale. However, there

are many uncalculable effects involving gravitons in the high energy theory and it is not clear that a common mass can still be maintained at low energies. Hence, we shall assume that the  $m_A$ 's are different in general. Hereafter, these parameters will carry subscripts denoting their particle species. Thus,  $m_N$ ,  $m_{H_1}$ ,  $m_{H_2}$  etc. will be the bare mass terms of the Higgs fields  $N$ ,  $H_1$ ,  $H_2$ , etc. respectively.

The gauge symmetry breaking is achieved by letting the three sets of Higgs fields,  $H_1$ ,  $H_2$  and  $N$  develop vacuum expectation values (VEV). Explicitly, we write

$$\langle H_1 \rangle = \begin{pmatrix} v_1/\sqrt{2} \\ 0 \end{pmatrix}, \quad (2.8a)$$

$$\langle H_2 \rangle = \begin{pmatrix} 0 \\ v_2/\sqrt{2} \end{pmatrix}, \quad (2.8b)$$

$$\langle N \rangle = v_3/\sqrt{2}. \quad (2.8c)$$

A set of constraint equations on the VEVs can then be obtained by minimizing the scalar potential contained in eq. (2.3)-(2.7). They are

$$m_{3/2} \left( \frac{3}{2} h v_1 v_2 + s \right) + \frac{v_3}{\sqrt{2}} \left( m_N^2 + \frac{h^2}{2} v^2 \right) = 0, \quad (2.9a)$$

$$\frac{3}{\sqrt{2}} m_{3/2} h v_2 v_3 + m_{H_1}^2 v_1 + \frac{h}{2} [h v_1 (v_2^2 + v_3^2) + 2s v_2] + \frac{1}{8} g^2 v_1 (v_1^2 - v_2^2) = 0 \quad (2.9b)$$

$$\frac{3}{\sqrt{2}} m_{3/2} h v_1 v_3 + m_{H_2}^2 v_2 + \frac{h}{2} [h v_2 (v_1^2 + v_3^2) + 2s v_1] - \frac{1}{8} g^2 v_2 (v_1^2 - v_2^2) = 0 \quad (2.9c)$$

where 
$$v^2 = v_1^2 + v_2^2, \quad (2.10)$$

and 
$$\bar{g}^2 = g^2 + g'^2. \quad (2.11)$$

In the limit that  $v_1 = v_2 \neq 0$ , taking the difference of eq. (2.9b) and (2.9c) gives

$$(m_{H_1}^2 - m_{H_2}^2) v_1 = 0. \quad (2.12)$$

Hence it is necessary for 'bare' masses of  $H_1$  and  $H_2$  to be equal if they were to develop the same VEV. The special case where  $v_1 = v_2 = a$  and  $m_{H_1} = m_{H_2} = m_N = m_{3/2}$  is solved in ref. 8. A particularly simple solution in this limit is given by

$$v_3 = \frac{-\sqrt{2}}{h} m_{3/2}, \quad (2.13a)$$

and 
$$a = \sqrt{2} \frac{m_{3/2}}{h} \left( 1 - \frac{sh}{m_{3/2}^2} \right)^{1/2}. \quad (2.13b)$$

Next we investigate the phenomenologically more interesting case of  $v_1 \neq v_2$ . For this case, the constraint equations can be recast into the following forms

$$\frac{3}{\sqrt{2}} m_{3/2} h v_3 - \frac{1}{4} g^2 v_1 v_2 + \frac{h}{2} (h v_1 v_2 + 2s) = \frac{m_{H_2}^2 - m_{H_1}^2}{v_2^2 - v_1^2} v_1 v_2 \quad (2.14a)$$

$$\frac{1}{2} (h^2 v_3^2 + \frac{1}{4} g^2 v_2^2) (v_1^2 - v_2^2) + m_{H_1}^2 v_1^2 - m_{H_2}^2 v_2^2 = 0, \quad (2.14b)$$

and 
$$\frac{3}{\sqrt{2}} h m_{3/2} v_3 + \frac{1}{2} h (h v_1 v_2 + 2s) + \frac{v_1 v_2}{v_2^2} (m_{H_1}^2 + h^2 v_3^2) = 0 \quad (2.14c)$$

which are useful in simplifying the mass matrix for the Higgs bosons. Eqs. (2.14) simplify for the case  $m_{H_1} = m_{H_2} = m$  in the non-degenerate VEV region. In particular eq. (2.14b) becomes

$$h^2 v_3^2 + 2m^2 = -\frac{1}{4} g^2 v^2 \quad (2.14b')$$

The three Higgs fields  $H_1$ ,  $H_2$  and  $N$  are not the physical mass eigenstates and a diagonalization has to be performed. There are six neutral spin-0 fields given by the real and the imaginary parts of the three fields; explicitly they are given by

$$H_1 = \begin{pmatrix} v_1 + \text{Re}H_1^0 + i\text{Im}H_1^0 \\ \sqrt{2} \\ H_2^+ \end{pmatrix}, \quad (2.15a)$$

$$H_2 = \begin{pmatrix} H_2^+ \\ \frac{v_2 + \text{Re}H_2^0 + i\text{Im}H_2^0}{\sqrt{2}} \end{pmatrix}, \quad (2.15b)$$

$$\text{and } N = \frac{1}{\sqrt{2}} (v_3 + \text{Re}N + i\text{Im}N). \quad (2.15c)$$

The superscripts on the H-fields are SU(2) indices. Two charged scalars form the following combinations:

$$H^+ \equiv \frac{1}{v} (v_1 H_2^+ + v_2 H_1^{2*}), \quad (2.16)$$

$$\text{and } G^+ \equiv \frac{1}{v} (v_2 H_2^+ - v_1 H_1^{2*}) \quad (2.17)$$

with  $H^-$  and  $G^-$  given by the conjugates of eq. (2.16) and (2.17). The physical charged Higgs fields are  $H^\pm$ , and  $G^\pm$  are the would-be-Goldstone-bosons which enter in the gauge-fixing conditions for the W-bosons given by

$$\partial_\mu W^{\mu+} = \frac{i\xi}{2\xi} v G^+, \quad (2.18a)$$

$$\text{and } \partial_\mu W^{\mu-} = \frac{i\xi}{2\xi} v G^-, \quad (2.18b)$$

where  $\xi$  is the gauge-fixing parameter. With the aid of  $M_W^2 = 1/4 g^2 v^2$  eq. (2.18) are seen to be the usual gauge conditions for the standard model. For the 't Hooft-Feynman gauge  $\xi=1$ . The combinations in eq. (2.16-17) can be shown to diagonalize the charge scalar mass matrix when the constraint equations of eq. (2.14) are used. The unphysical bosons  $G^\pm$  have mass  $M_W$  in the 't Hooft-Feynman gauge as expected. The mass of the physical charged scalars is given by

$$M_{H^\pm}^2 = h^2 v^2 + m_{H_1}^2 + m_{H_2}^2 + M_W^2 \quad (2.19)$$

for the general case of  $v_1 \neq v_2$ . Eq. (2.19) further limits the allowed values for  $m_{H_1}$  and  $m_{H_2}$ . One example is the case where  $v_1 \neq v_2$  and  $m_{H_1} = m_{H_2}$ . Using eq. (2.14b') we get

$$M_{H^\pm}^2 = -\frac{1}{4} g'^2 v^2 \quad (2.19')$$

Hence, if we want the effective Lagrangian of eq. (2.3-7) not to give unphysical charged Higgs bosons then  $m_{H_1} \neq m_{H_2}$  in the region where  $v_1 \neq v_2$

It is instructive to consider the case of degenerate VEV's, i.e.  $v_1 = v_2$ . We further simplify the discussion by the choice of

$$m_{H_1} = m_{H_2} = m_3/2 \quad (2.20)$$

and the solution of eq. (2.13a). Then we obtain

$$M_{H^\pm}^2 = 4m_3^2/2 + M_W^2 \quad (2.21)$$

Thus the simplest solutions lead to the conclusion that the charged Higgs boson is heavier than the W-boson quite independent of the coupling parameters in the scalar potential. We emphasize that this need not be true in general for  $v_1 \neq v_2$  and  $m_{H_1} \neq m_{H_2}$ .

The six neutral spin-0 bosons divide into scalars and pseudoscalars. One of the pseudoscalars is the would-be-Goldstone that is eaten up by the  $Z^0$ . This is given by

$$G^0 = \frac{1}{v} (v_2 \text{Im}H_2^0 - v_1 \text{Im}H_1^0). \quad (2.22a)$$

Orthogonal to  $G^0$  is a pseudoscalar  $h_0^0$ ; explicitly written as

$$h_0^0 = \frac{1}{v} (v_1 \text{Im}H_2^0 + v_2 \text{Im}H_1^0) \quad (2.22b)$$

and a third pseudoscalar  $\text{Im}N$ . In this basis  $G^0$  decouples from the

other two and only plays the role in  $Z^0$  gauge-fixing, i.e. terms like  $G^0 h_u^0$  and  $G^0 \text{ImN}$  are rotated away. However, the mass matrix of the two remaining  $O^-$  bosons is still not diagonal. Diagonalization can be achieved by the usual rotation and leads to the two physical pseudo-scalars,  $H_4^0$  and  $H_5^0$ , given by

$$H_4^0 = h_4^0 \cos x - \text{ImN} \sin x \quad (2.23a)$$

$$H_5^0 = h_4^0 \sin x + \text{ImN} \cos x. \quad (2.23b)$$

The mixing angle  $x$  can be obtained in terms of the parameters of the scalar potential via

$$\tan 2x = \frac{6h m_{3/2} v}{\sqrt{2} \{h^2 v^2 + (m_{H_1}^2 + m_{H_2}^2 - m_N^2)\}}. \quad (2.24)$$

In the degenerate VEV case with  $m_{H_1} = m_{H_2} = m_N = m_{3/2}$  and the solution (2.13a), we get

$$\tan 2x = \frac{\sqrt{2} h M_w}{8 m_{3/2}}. \quad (2.24')$$

Their masses are given by

$$M_4^2 = (h^2 v^2 + m_{H_1}^2 + m_{H_2}^2 + \frac{1}{2} h^2 v^2) \cos^2 x + \left(\frac{1}{2} h^2 v^2 + m_N^2\right) \sin^2 x + \frac{6}{\sqrt{2}} h m_{3/2} v \cos x \sin x \quad (2.25a)$$

$$M_5^2 = (h^2 v^2 + m_{H_1}^2 + m_{H_2}^2 + \frac{1}{2} h^2 v^2) \sin^2 x + \left(\frac{1}{2} h^2 v^2 + m_N^2\right) \cos^2 x - \frac{6}{\sqrt{2}} h m_{3/2} v \cos x \sin x \quad (2.25b)$$

and thus satisfy the sum rule

$$M_4^2 + M_5^2 = h^2 (v_3^2 + v^2) + m_{H_1}^2 + m_{H_2}^2 + m_N^2. \quad (2.26)$$

The remaining degrees of freedom are  $\text{Re}H_1^0$ ,  $\text{Re}H_2^0$  and  $\text{ReN}$  which are scalar ( $0^+$ ) fields and their mass matrix is again non-diagonal. We shall denote the physical mass eigenstates by  $H_i^0$  with eigenvalues  $M_i$  where  $i=1,2,3$  and these are obtained from the above by a unitary transformation,

$$H_i^0 = U_{ij} \text{Re}H_j^0. \quad (2.27)$$

In general the elements of  $U$  are complicated functions of the VEV's and the bare scalar masses, and are not particularly illuminating to examine. However, we note the following interesting sum rule

$$\sum_{i=1}^3 M_i^2 = M_4^2 + M_5^2. \quad (2.28)$$

Phenomenologically one can treat the  $U_{ij}$  as free parameters. From the above discussion we can also expect that these spin-0 bosons typically have masses of the order of  $M_w$  or  $m_{3/2}$  unless the parameters are wildly different.

Besides the mixing in the Higgs sector, the scalar fermions are also mixed. We focus our attention on the u-type squarks; in particular the scalar t-quarks since they are the only relevant ones in our calculations. A mixing between  $\tilde{t}_L$  and  $\tilde{t}_R$  which are distinct states arise from the last term in eq. (2.7b) when  $H_2$  develops a VEV. The mass matrix for  $\tilde{t}_L$  and  $\tilde{t}_R$  is given by

$$\begin{pmatrix} m_R^2 & m_t(m_{3/2} + \frac{h v_1}{v_2} v_3) \\ m_t(m_{3/2} + \frac{h v_1}{v_2} v_3) & m_L^2 \end{pmatrix} \quad (2.29a)$$

where

$$m_R^2 = \frac{1}{6} g'{}^2 (v_1^2 - v_2^2) + m_{DR}^2 \quad (2.29b)$$

and

$$m_L^2 = + \frac{1}{24} g'{}^2 (v_1^2 - v_2^2) (3g^2 + g'^2) + m_{BL}^2 \quad (2.29c)$$

with  $m_t$  being the t-quark mass and  $m_{B,R}(L)$  the bare mass appearing in  $\mathcal{L}_{SSB}$ . In general  $m_{BR}^2 \neq m_{BL}^2$ . From eq. (2.9a-c) we deduce that the mixing angle  $\tilde{\theta}$  between  $\tilde{L}_L$  and  $\tilde{L}_R$  is

$$\tan 2\tilde{\theta} = \frac{16m_{3/2}m_t}{8(m_{BR}^2 - m_{BL}^2) + (g'^2 - g^2)(v_1^2 - v_2^2)}. \quad (2.30)$$

In the symmetrical case of  $v_1 = v_2$  and  $m_{BR}^2 = m_{BL}^2$  then  $\tilde{\theta} = \pi/4$ . In general  $m_{BR}^2 \neq m_{BL}^2$  and  $v_1 \neq v_2$ . If we take  $m_R = m_{3/2}$  then  $\tilde{\theta}$  is of the order of  $\tan^{-1} \frac{m_t}{m_{3/2}}$ . Preliminary data from CERN [10] indicates that  $20 < m_t < 50 \text{ GeV}/c^2$  and it is possible that  $m_{3/2}$  can be a few times heavier than  $M_w$ . Thus,  $\tilde{\theta}$  is generally small even for the scalar t-quarks. For simplicity we shall ignore this mixing and treat  $\tilde{L}_L$  and  $\tilde{L}_R$  as mass eigenstates.

There is yet a third set of mixed states that are important in this calculation. These are states formed from the mixing of the winos and charged Higgsinos. In the Lagrangian [see eq. (2.2)] the charged gauginos and Higgsinos are represented by Majorana spinors  $\lambda^\pm$  and  $\psi_{H_1}^\pm$  and  $\psi_{H_2}^\pm$ , respectively with

$$\lambda^\pm = \frac{1}{\sqrt{2}} (\lambda_1^\pm + i\lambda_2^\pm). \quad (2.31)$$

Again they are not the physical mass eigenstates. These physical states are constructed explicitly as follows:

$$X_1 = \begin{pmatrix} -i\lambda^+ \cos\phi_+ + \psi_{H_2}^1 \sin\phi_+ \\ i\lambda^- \cos\phi_- + \psi_{H_1}^2 \sin\phi_- \end{pmatrix} \quad (2.32a)$$

and

$$X_2 = \begin{pmatrix} -i\lambda^+ \sin\phi_+ - \psi_{H_2}^1 \cos\phi_+ \\ -i\lambda^- \sin\phi_- + \psi_{H_1}^2 \cos\phi_- \end{pmatrix}. \quad (2.32b)$$

Notice that there are two separate mixing angles  $\phi_+$  and  $\phi_-$ .

One can read off from  $\mathcal{L}_{SSB}$  [see eq. (2.6)] and eq. (2.2) the mass terms involving the winos and charged Higgsinos. Diagonalization is achieved by eq. (2.32a,b). This procedure gives the mixing angle  $\phi_\pm$  and the masses  $\tilde{M}_1$  and  $\tilde{M}_2$  of the two physical chargino states  $X_1$  and  $X_2$  respectively. In terms of the parameters appearing in the Lagrangian, these angles are given by

$$\sin 2\phi_\pm = \frac{\tilde{m}}{\sqrt{2} M_w} \frac{[(1 + \sin 2\alpha)^{1/2} \pm (1 - \sin 2\alpha)^{1/2}]}{\left\{ \left( 1 + \frac{\tilde{m}^2}{2M_w^2} \right)^2 - \sin^2 2\alpha \right\}^{1/2}} \quad (2.33)$$

where  $\tan \alpha \equiv \frac{v_1}{v_2}$  (2.33')

This result is given in a different form in ref. [6]. For,  $v_2 \gg v_1$  or  $v_1 \gg v_2$  we have

$$\sin 2\phi_+ = \frac{\sqrt{2} \tilde{m}}{M_w \left( 1 + \frac{\tilde{m}^2}{2M_w^2} \right)} \quad (2.34a)$$

and  $\phi_- = 0$ . (2.34b)

On the other hand with equal VEV's we get  $\phi_+ = \phi_- = \phi$  and eq. (2.33) reduces to

$$\sin^2 2\phi = \frac{1}{\left( 1 + \frac{\tilde{m}^2}{4M_w^2} \right)} \quad (2.35)$$

The calculation also yields the masses  $\tilde{M}_1$  and  $\tilde{M}_2$ . These are written explicitly as

$$\tilde{M}_1 = \frac{1}{\sqrt{2}} M_w \left[ (1 + \sin 2\alpha + \frac{\tilde{m}^2}{2M_w^2})^{1/2} \pm (1 - \sin 2\alpha + \frac{\tilde{m}^2}{2M_w^2})^{1/2} \right]. \quad (2.36)$$

This completes the discussion on the physical states that appear in our calculations.

### 3. One loop calculation of $X^0 \rightarrow \gamma\gamma$

We use the Feynman rules listed in Appendix A to calculate the matrix elements which contribute to the two-photon decay widths of the  $X^0$  in the one-loop approximation. The internal loops for all of the scalar  $H_j^0$  decays consist of fermion and scalar fermions, gauge-bosons and gauginos and physical charged Higgs bosons. The would-be-Goldstone boson and Faddeev-Popov ghost loops are also included. The one-loop contribution to the two photon decays of the scalar  $H_j^0$  are displayed in six sets of diagrams in fig. 1. Each set is separately gauge invariant. Set 1 is the gauge boson loop contribution, denoted by  $a_{jW}$ , and includes mixed would-be-Goldstone bosons-gauge bosons and Faddeev-Popov ghosts. Set 2 is denoted by  $a_{jC}$  and consists only of full would-be-Goldstone boson loops. Both of these sets have the same structure as in standard model Higgs boson to two-photon decays [2]. As in the supersymmetric case [1], there are contributions from loops containing the physical charged Higgs boson,  $H^\pm$ , and the charginos,  $X_i^\pm$  ( $i=1,2$ ). These are sets 3 and 4, contributing amounts  $a_{jH}$  and  $a_{jX_i}$  respectively. If the Yukawa couplings are non-vanishing then the fermion loops of set 5 will give the  $a_{jF}$ . Finally set 6 shows the scalar-fermion contribution  $a_{j\tilde{f}}$ , which contains both gauge and Yukawa pieces. As noted in the previous section, the small mixing between left and right types of scalar-fermions has been neglected for simplicity. Combining all the contributions, we find the matrix elements for the scalar  $H_j^0$  ( $j=1,2,3$ ) decays into two photons with polarization vectors  $e_\mu^{(1)}$  and  $e_\nu^{(2)}$  to be

$$a_j = (a_{jW} + a_{jC} + a_{jX_1} + a_{jX_2} + a_{jH} - a_{jF}) N^{\mu\nu} e_\mu^{(1)} e_\nu^{(2)} \quad (3.1)$$

$$\text{with } a_{jW} = \frac{ie^2 g_{M_W}}{(4\pi)^2} [6 + (-8 + 12\lambda_w) I(\lambda_w)] \left[ \frac{v_{1j} U_{1j} + v_{2j} U_{2j}}{v} \right] \quad (3.2)$$

$$a_{jC} = \frac{ie^2 g_{M_W}^2}{(4\pi)^2 M_W} [1 + 2\lambda_w I(\lambda_w)] \left[ \frac{v_{1j} U_{1j} + v_{2j} U_{2j}}{v} \right] \quad (3.3)$$

$$a_{jX_1} = - \frac{2\sqrt{2} ie^2 g_{M_1}^2}{(4\pi)^2} [2 + (4\lambda_1 - 1) I(\lambda_1)] [s_{\mp c} c_{\pm} U_{1j} + s_{\pm c} c_{\mp} U_{2j}] \quad (3.4)$$

$$a_{jH} = \frac{2ie^2 g_{M_W}}{(4\pi)^2} [1 + 2\lambda_H I(\lambda_H)] \left[ \left(1 - \frac{1}{2} \lambda_w^{-1}\right) \left(\frac{v_{1j} U_{1j} + v_{2j} U_{2j}}{v}\right) + \frac{2h^2 v_{3j} U_{3j}}{g_{M_W}} \right] \quad (3.5)$$

$$a_{jF} = - \sum_f \frac{2ie^2 e_f^2 m_f^2 c_f v}{(4\pi)^2 M_W} [2 + (4\lambda_f - 1) I(\lambda_f)] v_f \quad (3.6)$$

$$a_{j\tilde{f}} = - \sum_f \frac{2ie^2 e_f^2 c_f}{(4\pi)^2} [1 + 2\lambda_{\tilde{f}} I(\lambda_{\tilde{f}})] \left[ \frac{g^2 (v_{2j} U_{2j} - v_{1j} U_{1j})}{2 \cos^2 \theta_w} \frac{N_{\tilde{f}}^L(R) - 2m_{\tilde{f}}^2 v_f}{N_{\tilde{f}}^L(R)} \right], \quad (3.7)$$

$$\text{where } v_f(\tilde{f}) = \frac{1}{v_1} U_{1j} \text{ for } f=d\text{-fermions (sfermions)} \quad (3.8a)$$

$$= \frac{1}{v_2} U_{2j} \text{ for } f=u\text{-fermions (sfermions)} \quad (3.8b)$$

Furthermore,

$$N_{\tilde{f}}^L = \frac{1}{2} \eta_f - e_f \sin^2 \theta_w, \quad N_{\tilde{f}}^R = e_f \sin^2 \theta_w \quad (3.9)$$

$$\text{and } \lambda = m^2 / M_j^2 \quad (3.10)$$

The subscript of the  $\lambda$ 's corresponds to the mass of the internal loop particle. Here  $\eta_f$  is  $+1(-1)$  for up (down) type sfermions. Also  $s_{\pm c}$  denote  $\sin\phi_{\pm}$ ,  $\cos\phi_{\pm}$  respectively [see eq. (2.32)]. The color factor  $c_f$  is 3 for quarks and 1 for leptons. The gauge invariant quantity  $N_{\mu\nu}$  is



$$N_{\mu\nu} = \left[ g_{\mu\nu} - \frac{p_\nu q_\mu}{p \cdot q} \right] \quad (3.11)$$

where  $p$  and  $q$  are the photon momenta, of the first and second photon respectively, and

$$I(\lambda) = \int_0^1 dx \frac{1}{x} \ln \left[ 1 - \frac{1}{\lambda} x(1-x) \right]. \quad (3.12)$$

We note that the function  $\lambda I(\lambda)$  has a very weak dependence on  $\lambda$  for values of  $\lambda \gg 1/4$ . This is shown in fig. 2.

Similarly we computed the matrix elements for the two-photon decays of the pseudoscalars  $H_u^0$  and  $H_s^0$ . The diagrams which contribute are displayed in fig. 3, and consist only of fermion and gaugino loops. We find the matrix elements for the pseudoscalar  $H_k^0$  ( $k=4,5$ ) to be

$$a_k = \left( a_{kX_1} + a_{kX_2} \right) N_{ps}^{\mu\nu} (1) e_\nu^y \quad (3.13)$$

with

$$a_{kX_1} = \frac{4\sqrt{2} e^2 g_{M_1}^2}{(4\pi)^2 v} \left( v_2 s_\tau^2 c_\tau^2 + v_1 s_\tau^2 c_\tau^2 \right) I(\lambda_1) \eta_k \quad (3.14)$$

$$a_{kF} = - \sum_F \frac{4e^2 g_3^2 g_{M_1}^2 c_F}{(4\pi)^2 M_W} \left( \frac{v_1}{v_2} \right) \eta_F I(\lambda_F) \eta_k \quad (3.15)$$

where

$$N_{ps}^{\mu\nu} = \epsilon^{\mu\nu\rho\omega} \frac{p_\rho q_\omega}{2p \cdot q} \quad (3.16)$$

and  $\eta_k$  is  $\cos x(\sin x)$  for  $k=4(5)$ .

The above gives the general amplitudes for scalar or pseudoscalar Higgs boson to two-photon decays in broken supersymmetric theory, calculated with component field techniques. Obviously these amplitudes contain many unknown parameters such as mixing angles and masses of unseen particles. In the next section we shall make some reasonable

simplifying assumptions and estimate the widths. We shall examine carefully the allowed enhancement of these widths in broken supersymmetric gauge theories.

#### 4. Widths of $X^0 + \gamma\gamma$

The widths of  $X^0 + \gamma\gamma$  can now be trivially calculated from the results presented in the last section. However, we have to fix or establish a range for the many parameters appearing in the amplitudes. We discuss two extreme cases for the ratio of the two VEV's  $v_1$  and  $v_2$ . We shall call  $v_1 \gg v_2$  case A and  $v_1 = v_2$  case B.

We begin with the pseudoscalar  $H_u^0$  and  $H_s^0$  decays. For case A, the mixings of the charginos are given by eq. (2.33). Substituting into eq. (3.15) and (3.16), we find the dominant contributions come from  $X_1$  and the  $t$ -quark; thus for  $H_u^0$  decays

$$a_{X_1} = \frac{\sqrt{2} e^2 g_{M_1}^2}{4\pi^2} \frac{I(\lambda_{X_1})}{M_W} \cos x \sin \phi + \quad (4.1)$$

$$a_t = - \frac{e^2 g}{3\pi^2} M_W \tan \alpha \frac{m_t^2}{M_W^2} I(\lambda_t) \cos x. \quad (4.2)$$

From eq. (2.24) we do not discern any reason why the mixing between the pseudoscalars should be small. Hence, we expect  $\cos x \approx 1/\sqrt{2}$ . Notice that the relative phases of  $a_t$  and  $a_{X_1}$  are destructive since  $\phi + \pi$  is in the first quadrant. The width for  $H_u^0$  decays can be trivially obtained to be

$$\Gamma(H_u^0 \rightarrow \gamma\gamma) = \frac{\alpha^3 M_2^2 \cos^2 x}{(4\pi)^2 \sin^2 \theta M_W} \left[ \sqrt{2} \frac{M_1}{M_W} I(\lambda_{X_1}) \sin \phi + \frac{4}{3} \tan \alpha \frac{m_t^2}{M_W^2} I(\lambda_t) \right]^2 \quad (4.3)$$

The width of  $H_s^0$  decay is obtained from the above by substituting  $\sin x$  for  $\cos x$  and  $M_u$  by  $M_s$ .

At first sight, bounds on the magnitude of  $\tan\alpha$  can be determined by low energy phenomenology just as in the two Higgs doublet model. This is achieved by examining constraints from Bhabha scattering, muon decays [10,11,12] and  $K_{OL}^-K_{OS}$  mass difference [13]. Taken together these considerations give

$$\tan\alpha < 40. \quad (4.4a)$$

Moreover, if we also take into account partial wave unitarity plus perturbation theory [14], one gets the more stringent bound of

$$\tan\alpha < 12. \quad (4.4b)$$

In supersymmetry there is a further constraint on  $\tan\alpha$ . This is due to the relation between the masses,  $\tilde{M}_1$  and  $\tilde{M}_2$ , and  $\tan\alpha$ . From eq. (2.35) we have

$$\tilde{M}_1 = \frac{M_W}{2} \left[ \left( 1 + \sin 2\alpha + \frac{\tilde{m}^2}{2M_W^2} \right)^{1/2} \pm \left( 1 - \sin 2\alpha + \frac{\tilde{m}^2}{2M_W^2} \right)^{1/2} \right]. \quad (4.5)$$

For the case of interest, we can prove that,

$$\tan\alpha = \frac{2M_W^2}{\tilde{M}_1 \tilde{M}_2} \quad (4.6)$$

As can be seen in eq. (4.5),  $\chi_2$  is the lighter of the two charginos. It must have a mass greater than 20 GeV/c<sup>2</sup>, otherwise the width of W-boson decaying into  $\chi_2$  and  $\tilde{\gamma}$  will exceed 5 GeV [15]. This then puts

$$\tan\alpha < \frac{8M_W}{\tilde{M}_1} \quad (4.4c)$$

for  $M_W=80$  GeV/c<sup>2</sup> and  $\tilde{M}_2 > 20$  GeV/c<sup>2</sup>. Hence in order to remain in case A,  $\chi_1$  must have a mass no more than  $\sim 7$  times  $M_W$ . The consistent range for  $\tilde{M}_1$  would be  $1/2 M_W < M_1 \lesssim 7 M_W$ .

In fig. 4 we display the width of  $H_u^0$  decaying into two photons as a function of its mass, for the range of allowed  $\chi_1$  masses, with the mixing angle  $x$  chosen to be  $\pi/4$ . It is seen that this width is typically of the order of 60 keV or less for an intermediate mass pseudoscalar.

The width is dominated in this case by the t-quark loop contribution. The dependence of  $\tan\alpha$  via eq. (4.4c) on the  $\chi_1$  mass is the reason for the large range of possible widths for a given pseudoscalar mass. As the pseudoscalar mass approaches and then crosses the threshold for decay into a pair of real t-quarks ( $m_t=40$  GeV/c<sup>2</sup>), the rise in the width respectively increases sharply and then slows abruptly. In general this type of behaviour will occur whenever the threshold for pair production of a particle which makes an important loop contribution to the decay width is crossed. Similar result holds for  $H_S^0$  decays. Next we examine case B. With  $\alpha = \pi/4$  we obtain again  $\phi_+ = \phi_- = \phi$  and explicitly

$$\phi = \frac{1}{2} \sin^{-1} \frac{1}{\left( 1 + \frac{\tilde{m}^2}{4M_W^2} \right)^{1/2}} \quad (4.7)$$

The masses of the charginos are given by

$$\tilde{M}_{1,2} = M_W \left\{ \left( 1 + \frac{\tilde{m}^2}{4M_W^2} \right)^{1/2} \pm \frac{\tilde{m}}{2M_W} \right\} \quad (4.8)$$

and they are the order of  $M_W$ . Now the two-photon widths of  $H_u^0$  and  $H_S^0$  are easily obtained to be

$$\Gamma(H_u^0 + \gamma\gamma) = \frac{\alpha^3 M_W^2 \cos^2 x}{(4\pi)^2 \sin^2 \theta_W M_{H_u^0}} \left[ \frac{\tilde{M}_1}{M_W} I(\chi_{\chi_1}) + \frac{\tilde{M}_2}{M_W} I(\chi_{\chi_2}) \right] \left[ \sin 2\phi - \frac{4}{3} \frac{m_t^2}{M_W^2} I(\lambda_t) \right]^2 \quad (4.9)$$

and substituting  $\sin^2 x$  for  $\cos^2 x$  and  $M_5$  for  $M_4$  to get  $\Gamma(H_S^0 + \gamma\gamma)$ .

These widths as a function of their mass, for the range of allowed chargino masses, are plotted in fig. 5. Neither  $\chi_1$ ,  $\chi_2$  nor the t-quark loop contributions dominate, since there is no tan enhancement. Consequently the width is much smaller than in case A, i.e. less than 25 keV. The upper bound curve in fig. 5 corresponds to both charginos having mass  $M_w$ , and hence is sharply peaked near the threshold at  $2M_w$ .

It is now straightforward to carry out the same analysis for the two-photon widths of the scalar Higgs bosons  $H_j^0$  ( $j=1,2,3$ ). For definiteness we discuss only  $H_1^0$  decays. It is clear that the same analysis can be pushed through almost verbatim for  $H_2^0$  and  $H_3^0$ . Just as in the case of the pseudoscalars there is no apparent reason for the mixing  $U_{ij}$  between these scalars to be small. For simplicity we assume that they are all approximately equal, i.e.  $U_{1j}=U_{2j}=U_{3j}=U=1/\sqrt{3}$  for  $j=1,2,3$ .

As seen in fig. 1 there are many more internal loop contributions compared to pseudoscalars; hence, more free parameters in the form of internal masses appear. We already noted that the combination  $\lambda I(\lambda)$  does not vary a great deal over a wide range of values for  $\lambda$ . Thus, we do not expect the two-photon widths to be too sensitive to the values we choose for these masses.

Observe that the amplitude due to fermion loops of eq. (3.6) is dominated by the t-quark for both cases A and B. This is due to the mass of the t-quark being much larger than other fermions in the minimal 3 quark-lepton families universe. For case A further enhancement is due to the presence of the  $V_f$  factor. Notice that the scalar-fermion loop contribution of eq. (3.7) is dominated by the scalar-top for both cases A and B. To the extent that  $\lambda_c I(\lambda_c)$  is insensitive to the choice of scalar fermion mass, the term involving  $N_{L(R)}^f$  will give zero when summed over

all scalar fermion types. The remaining Yukawa term is proportional to the square of the corresponding fermion mass, and hence the scalar-top dominates. Again in case A there is further enhancement by the  $V_f^2$  factor.

Incorporating the above considerations, we find that for case A the scalar decays have

$$a_w = \frac{1e^2 g M_w}{(4\pi)^2} [6 + (-8+12\lambda_w) I(\lambda_w)] U \quad (4.10)$$

$$a_G = \frac{1e^2 g M_w}{(4\pi)^2} [\lambda_w^{-1} + 2I(\lambda_w)] U \quad (4.11)$$

$$a_{\chi_1^0} = \frac{-2\sqrt{2}1e^2 \tilde{g} M_1}{(4\pi)^2} \left[ \frac{2}{2} + (4\lambda_1 - 1) I(\lambda_1) \right] U \sin\theta + \quad (4.12)$$

$$a_H = \frac{21e^2 M_w}{(4\pi)^2} [1 + 2\lambda_H I(\lambda_H)] \left[ \left( 1 - \frac{1}{2} \lambda_w^{-1} \right) + \frac{2H^2 V_3}{g M_w} \right] U \quad (4.13)$$

$$a_t = - \frac{81g e^2 w_t^2}{3(4\pi)^2 M_w} [2 + (4\lambda_t^{-1}) I(\lambda_t)] U \tan\alpha \quad (4.14)$$

$$a_c^c = \frac{161e^2 g m_c^2}{3(4\pi)^2 M_w} [1 + 2\lambda_c I(\lambda_c)] U \tan\alpha \quad (4.15)$$

to give a width of

$$\Gamma(H^0 + \gamma\gamma) = \frac{1}{16\pi M} |a_w^+ a_G^+ a_{\chi_1^0}^+ a_t^+ a_H^+ a_c^+ a_c^c|^2 \quad (4.16)$$

This width as a function of the scalar mass is displayed in fig. 6. The standard model scalar width is also shown for comparison. The major contributions to the scalar width in this mass range are the t-quark loop, W-gauge boson loop, and to a smaller extent the chargino loops. For larger scalar masses, the scalar-top and charged Higgs loops will also

contribute, but only near or above their thresholds. Destructive interference between the t-quark and W-gauge boson loops results in a generally smaller width than in the standard model which by comparison is dominated only by the W-gauge boson loop. All the curves in fig. 6 rise sharply near 160 GeV/c<sup>2</sup>, which corresponds to the threshold for W-gauge boson pairs.

Similarly for case B we have

$$a_W = \frac{ie^2 g_{M_W}^2}{(4\pi)^2} [6 + (-8+12\lambda_W)I(\lambda_W)] \sqrt{2} U \quad (4.17)$$

$$a_G = \frac{ie^2 g_{M_W}^2}{(4\pi)^2} [\lambda_W^{-1} + 2I(\lambda_W)] \sqrt{2} U \quad (4.18)$$

$$a_{\chi_1^0} = \frac{-2\sqrt{2}ie^2 g_{M_W}^2}{(4\pi)^2} \left[ 2 + \left( 4\lambda_1^{-1} - 1 \right) I\left(\lambda_1\right) \right] U \sin 2\phi \quad (4.19)$$

$$a_H = \frac{2ie^2 g_{M_W}^2}{(4\pi)^2} [1+2\lambda_H I(\lambda_H)] \left[ \left( 1 - \frac{1}{2} \lambda_W^{-1} \right) \sqrt{2} + \frac{2h^2 v_3}{g_{M_W}} \right] U \quad (4.20)$$

$$a_t = \frac{-81ge^2 m_t^2}{3(4\pi)^2 M_W} [2 + (4\lambda_t^{-1} - 1)I(\lambda_t)] \sqrt{2} U \quad (4.21)$$

$$a_{\tau} = \frac{16ie^2 g_{M_W}^2}{3(4\pi)^2 M_W} [1 + 2\lambda_{\tau}^{-1} I(\lambda_{\tau})] \sqrt{2} U \quad (4.22)$$

Substituting these into eq. (4.16) gives the width  $\Gamma(H^0 \rightarrow \gamma\gamma)$  which we again display as a function of scalar mass in fig. 7. Once again the standard model width is shown for comparison. The discussion is similar to that for case A, except that the t-quark loop is not an important contribution here, since there is no tan $\alpha$  enhancement. Consequently the width is a bit larger, and dominated mostly by the W-gauge boson loop.

The gaugino loops interfere destructively with the W-gauge boson loop and hence the scalar width is still smaller than in the standard model.

Finally we note that thus far we have used the example where the mixings  $U_{ij}$  are all approximately equal. We now consider the best case possibility, where the relative phases between mixings is such that the dominant loop contributions interfere constructively. This is not possible in case B since the gauge boson and gaugino loops contain the same combinations of  $U_{ij}$  with an overall relative minus sign. However, for case A we can greatly increase the width if  $U_{1j} = U_{2j}$ . This will give constructive rather than destructive interference between the two main contributors, namely the gauge-boson and t-quark loops. The scalar width for this best case scenario is plotted in fig. 8, and it is indeed now enhanced relative to the standard model width, although not by a great amount.

## 5. Conclusions

We have calculated the two-photon decay widths for Higgs scalar and pseudoscalar bosons in a minimal broken supersymmetry model. Being an example of a model with two Higgs doublets with added theoretical motivation, it has all the features associated with such models. First there are the scalar and pseudoscalar bosons which are in addition to the usual standard model Higgs scalar. Second there is the possibility of enhanced couplings to these bosons relative to the standard model, if the ratio of the two VEV's, tan $\alpha$ , is large. In addition to these two general points, the model studied has new features associated with the underlying albeit broken supersymmetry. Specifically the charged gauginos and scalar-fermions will give additional loop contributions to the two-photon decay widths. In the intermediate mass range studied (40-160 GeV/c<sup>2</sup>), we found

that these additional contributions are not very large and in fact they in general reduce the width by interfering destructively with the usual contributions. One important additional feature arising from the supersymmetry is the upper bound imposed on  $\tan\alpha$  by the allowed range of the gaugino masses. The upper limit of  $\tan\alpha \lesssim 5.6$  in the minimal broken supersymmetry model is less than half of the most restrictive bound for a general two-Higgs doublet model. The width varies as  $\tan^2\alpha$  for large  $\tan\alpha$ , so that the largest possible width for this model is at least 4 times smaller than one might have hoped for. A more optimistic situation can arise if the mixings between the scalars, coming from the breaking of the supersymmetry, have phases such that constructive interference occurs between the  $W$ -gauge boson and  $t$ -quark loops. In this case the scalar width is enhanced to partially compensate for the smaller  $\tan\alpha$  factor. Even this best case possibility allows an enhancement of the scalar width of less than an order of magnitude over the standard model width. For the pseudoscalar this best case possibility does not occur since the relative phases are fixed, and hence the pseudoscalar width is definitely smaller. Hence, we conclude that the supersymmetry imposes a much lower upper bound on the possible  $\tan\alpha$  enhancement of the two photon decay widths than do two Higgs doublet models in general. Widths of the order of 100 keV is the best one can hope for both scalars and pseudoscalars in the minimal broken supersymmetric gauge theory.

## References

- [1] P. Kalyniak, R. Bates, and J.N. Ng, TRIUMF preprint (1985) TRI-PP-85-77.
- [2] R. Bates and J.N. Ng, TRIUMF preprint (1985) TRI-PP-85-57.
- [3] M.K. Sundaresan and P.J.S. Watson, Phys. Rev. Lett. 29 (1972) 15; J. Ellis, M.K. Gaillard, and D.V. Nanopoulos, Nucl. Phys. B106 (1976) 292;
- L.H. Chan and T. Hagiwara, Phys. Rev. D20 (1979) 1698.
- [4] L. Hall, J. Lykken, and S. Weinberg, Phys. Rev. D27 (1983) 2359; A.H. Chamesddine, R. Arnowitt, and P. Nath, Phys. Rev. Lett. 49 (1982) 970;
- For a review see H.P. Nilles, Phys. Rept. 110C (1984) 1.
- [5] L. Girardello and M.T. Grisaru, Nucl. Phys. B194 (1982) 65.
- [6] P. Fayet, Nucl. Phys. B90 (1975) 104.
- [7] H. Haber and G. Kane, Phys. Rept. 117C (1985) 76.
- [8] E. Cremmer, P. Fayet, and L. Girardello, Phys. Lett. 122B (1982) 41.
- [9] R. Barbieri, S. Ferrara, and C.A. Savoy, Phys. Lett. 119B (1982) 343.
- [10] A. Arnison et al., UAI Collaboration, Phys. Lett. 147B (1984) 493.
- [11] H.E. Haber, G.L. Kane and T. Sterling, Nucl. Phys. B161 (1979) 493.
- [12] J.N. Ng, Phys. Rev. D31 (1985) 464.
- [13] L.F. Abbot, P. Sikivie, and M.B. Wise, Phys. Rev. D21 (1980) 1393.
- [14] M.S. Chanowitz, M.A. Furman and I. Hinchliffe, Nucl. Phys. B153 (1979) 402.
- [15] V. Barger, R.W. Robinett, W.Y. Leung, and R.J.N. Phillips, Phys. Rev. D28 (1983) 233.

- [16] J. Wess and B. Zumino, Phys. Lett. 49B (1974) 52.
- [17] B. deWit and D.Z. Freedman, Phys. Rev. D12 (1975) 2286.
- [18] J. Gunion and H. Haber, SLAC-PUB-3404 (1984).

### Appendix A: Feynman Rules

The effective Lagrangian for broken supersymmetric standard models is given in eq. (2.1)-(2.7) in component fields. The component field content of the theory is displayed in table 1. In working with component fields we have chosen the usual Wess-Zumino gauge of supersymmetry [16]. The gauge of the  $SU(2) \times U(1)$  symmetry is fixed to be the 't Hooft-Feynman gauge. The ghost is thus the same as that of the standard model [17]. We have explicitly calculated the Faddeev-Popov (FP) Lagrangian. Due to the mixing of the scalars all three fields  $H_j^0$ ,  $j=1,2,3$  couple to the ghost field. As expected the pseudoscalars  $H_u^0$  and  $H_s^0$  do not couple to the FP ghosts.

The relevant couplings for the calculation of the amplitudes of  $X^0 + \gamma\gamma$  are given in different sets below. The first set involves the scalar couplings to fermion, sfermions, charged Higgs bosons  $H^\pm$  and their companion would-be-Goldstone bosons,  $G^\pm$ , as well as the gauge bosons  $W^\pm$  and the FP ghosts. This is displayed in fig. (A1). Fig. (A2) gives all the photon couplings. The mixed states of charged Higgsinos and winos,  $X_1$  and  $X_2$ , have couplings to the Higgs scalars given in fig. (A3). Sewing together the vertices given above gives the full set of Feynman diagrams displayed in fig. (1) for  $H_j^0$  to two photon decays.

For the pseudoscalars the couplings are simpler. Only two are relevant; namely  $X_1$  and  $X_2$  and fermion couplings are involved and these are represented in fig. (A4).

Some of the above rules are given in ref. [18]. However, the authors there worked in the unitary gauge. For couplings that do not depend on the gauge chosen we have found agreement.

Table 1

Field content of the minimal supersymmetric SU(2) $\times$ U(1) model with one family. SU(2) gauge bosons carry the label a=1,2,3 and the matter fields have the SU(2) Index i=1,2. The last two columns give the SU(2) representations and the U(1) hypercharges of the respective fields. The superscript c indicates charge conjugation.

Gauge Bosons	Gauginos	SU(2)	Y
$v^a$	$\chi^a$	1	0
$v^i$	$\lambda^i$	0	0
Leptons	Sleptons		
$L_L^i=(\nu, e^-)_L$	$\tilde{L}_L^i=(\tilde{\nu}, \tilde{e}^-)_L$	1/2	-1
$e_L^c$	$\tilde{e}_R^+$	0	2
Quarks	Squarks		
$Q_L^i=(u, d)_L$	$\tilde{Q}_L^i=(\tilde{u}_L, \tilde{d}_L)_L$	1/2	1/3
$u_L^c$	$\tilde{u}_R^*$	0	-4/3
$d_L^c$	$\tilde{d}_R^*$	0	2/3
Higgs Bosons	Higgsinos		
$H_1^1$	$(\psi_{H_1}^1, \psi_{H_1}^2)$	1/2	1
$H_2^1$	$(\psi_{H_2}^1, \psi_{H_2}^2)$	1/2	1
$N$	$\psi_N$	0	0

Figure Captions

1. One-loop contributions to the two photon decay of the scalar  $H_j^0$  ( $j=1,2,3$ ). The diagrams are grouped into separately gauge invariant sets. (I) gauge boson, would-be-Goldstone boson, and ghost loops (II) would-be-Goldstone boson loops (III) physical charged Higgs boson loops (IV) charginos loops (V) fermion loops (VI) scalar-fermion loops.
2. Plot of the function  $\lambda I(\lambda)$  vs.  $\lambda$ . The solid (broken) curve shows the real (imaginary) part.
3. One-loop contributions to the two photon decay of the pseudoscalar  $H_k^0$  ( $k=4,5$ ). (I) chargino loops (II) fermion loops.
4. Case A ( $v_1 \gg v_2$ ): two photon decay width as a function of mass for the pseudoscalar  $H_k^0$  ( $k=4,5$ ) with mixing angle  $x=\pi/4$ , for the range of allowed  $\chi_1$  masses.
5. Case B ( $v_1=v_2$ ): two photon decay width as a function of mass for the pseudoscalar  $H_k^0$  ( $k=4,5$ ) with mixing angle  $x=\pi/4$ , for the range of allowed  $\chi_1$  masses.
6. Case A ( $v_1 \gg v_2$ ): Two photon decay width as a function of mass for the scalar  $H_j^0$  ( $j=1,2,3$ ) with mixing angles  $U_{1j}=U_{2j}=U_{3j}=1/\sqrt{3}$ , for the range of allowed  $\chi_1$  masses. The broken curve shows the standard model Higgs boson width for comparison.
7. Case B ( $v_1=v_2$ ): two photon decay width as a function of mass for the scalar  $H_j^0$  ( $j=1,2,3$ ) with mixing angles  $U_{1j}=U_{2j}=U_{3j}=1/\sqrt{3}$ , for the range of allowed  $\chi_1$  masses. The broken curve shows the standard model Higgs boson width for comparison.
8. Case A ( $v_1 \gg v_2$ ): two photon decay width as a function of mass for the scalar  $H_j^0$  ( $j=1,2,3$ ) with mixing angles  $U_{1j}=-U_{2j}=U_{3j}=1/\sqrt{3}$ , for the

range of allowed  $X_1$  masses. The broken curve shows the standard model Higgs boson width for comparison.

A1. Feynman rules for scalar  $H_j^0$  ( $j=1,2,3$ ) couplings in the

't Hooft-Feynman gauge. Here  $V_f^f(\vec{f})$  and  $N_{R/L}^f$  are defined in

Eqs. (3.8) and (3.9).

A2. Feynman rules for photon couplings in the 't Hooft-Feynman gauge.

A3. Feynman rules for chargino-scalar  $H_j^0$  ( $j=1,2,3$ ) couplings.

A4. Feynman rules for chargino-pseudoscalar  $H_k^0$  ( $k=4,5$ ) couplings. Here

$\eta_f = +1(-1)$  for up (down) type fermions, and  $\eta_k = \cos x$  ( $\sin x$ ) for

$k=4(5)$ .

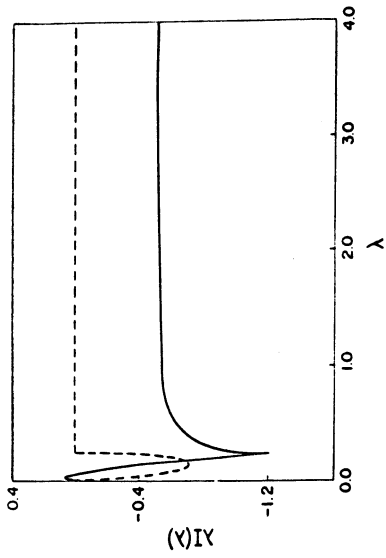


Fig. 2

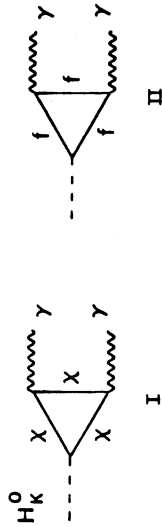


Fig. 3

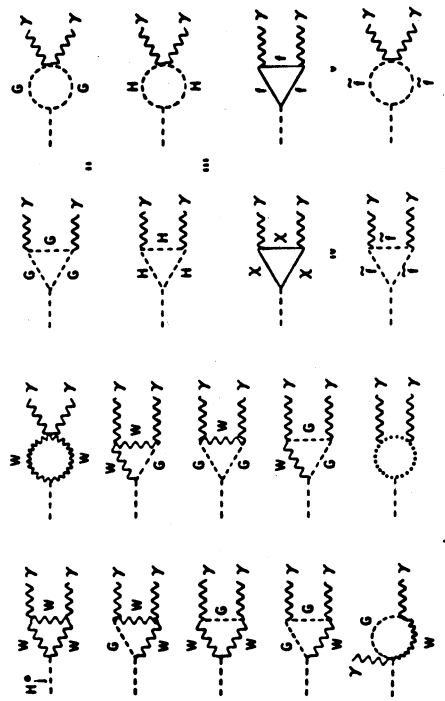


Fig. 4

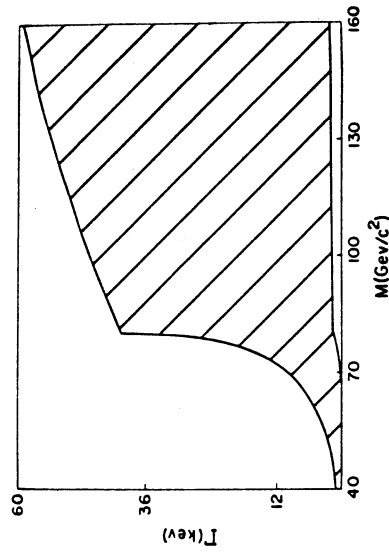


Fig. 4



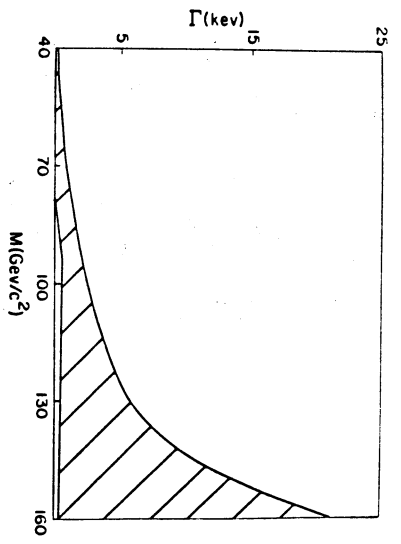


Fig. 5

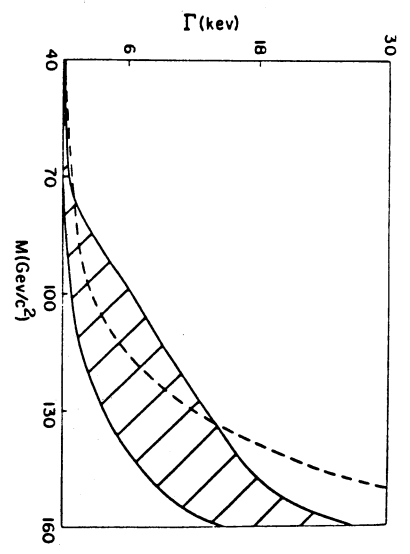


Fig. 6

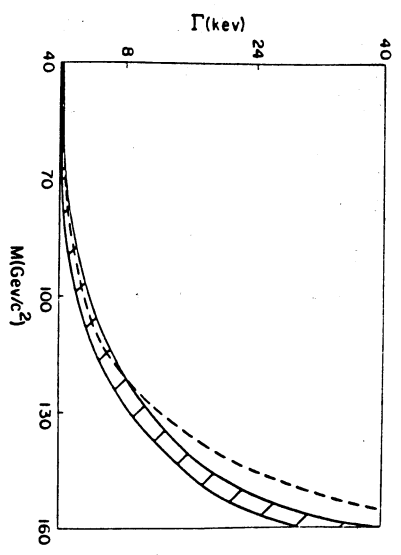


Fig. 7

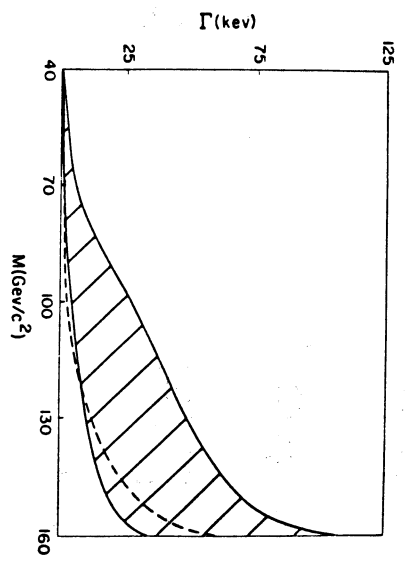


Fig. 8

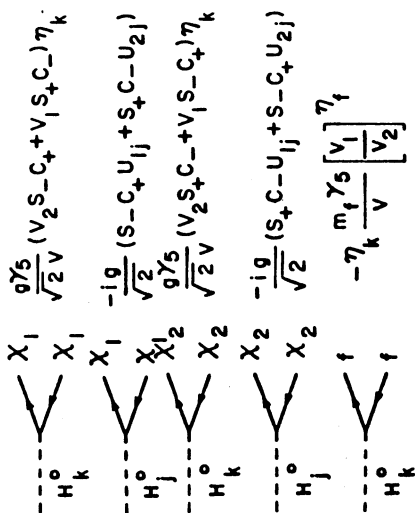


Fig. A3

$$\frac{g\gamma_5}{\sqrt{2}V} (V_2 S_{-C_+} + V_1 S_{+C_-}) \eta_k$$

$$-\frac{ig}{\sqrt{2}} (S_{-C_+} U_{1j} + S_{+C_-} U_{2j})$$

$$\frac{g\gamma_5}{\sqrt{2}V} (V_2 S_{+C_-} + V_1 S_{-C_+}) \eta_k$$

$$-\frac{ig}{\sqrt{2}} (S_{+C_-} U_{1j} + S_{-C_+} U_{2j})$$

$$-\eta_k \frac{m_f \gamma_5}{V} \begin{bmatrix} V_1 \\ V_2 \end{bmatrix} \eta_f$$

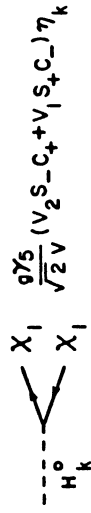


Fig. A4

$$\frac{g\gamma_5}{\sqrt{2}V} (V_2 S_{-C_+} + V_1 S_{+C_-}) \eta_k$$

$$\frac{g\gamma_5}{\sqrt{2}V} (V_2 S_{+C_-} + V_1 S_{-C_+}) \eta_k$$

$$-\eta_k \frac{m_f \gamma_5}{V} \begin{bmatrix} V_1 \\ V_2 \end{bmatrix} \eta_f$$

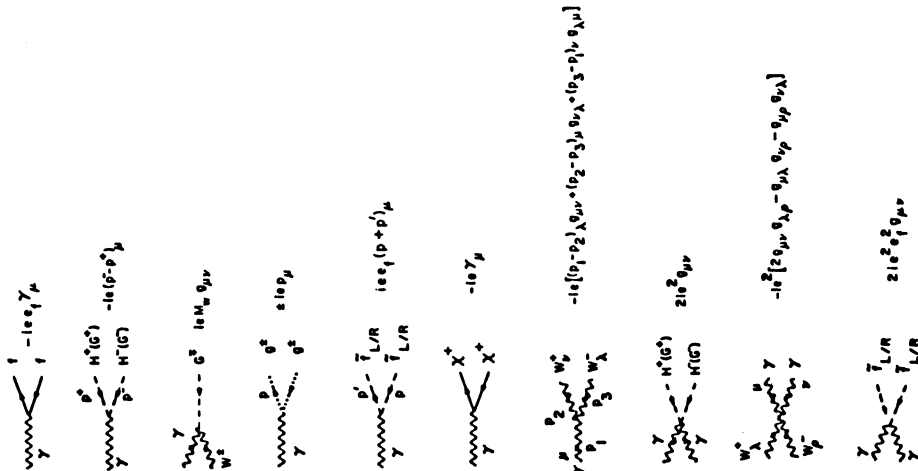


Fig. A2

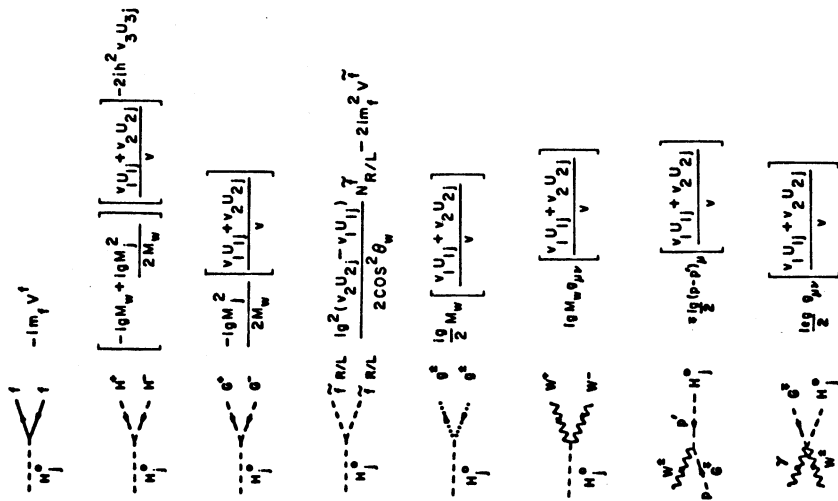


Fig. A1

$$-im_f v^f$$

$$\frac{-igM_w + igM^2}{2M_w} \left[ \frac{v_{U_1} + v_{U_2}}{v} \right] \left[ \frac{v_{U_1} + v_{U_2}}{v} \right] - 2in^2 v_{U_1} v_{U_2}$$

$$-\frac{igM^2}{2M_w} \left[ \frac{v_{U_1} + v_{U_2}}{v} \right]$$

$$\frac{\tilde{T} R/L}{2 \cos^2 \theta_w} \frac{ig^2 (v_{U_2} - v_{U_1})}{2} \frac{\gamma}{R/L} - 2im_f^2 v^f$$

$$\frac{ig}{2} M_w \left[ \frac{v_{U_1} + v_{U_2}}{v} \right]$$

$$ig M_w \rho_{\mu\nu} \left[ \frac{v_{U_1} + v_{U_2}}{v} \right]$$

$$\frac{ig}{2} \rho_{\mu\nu} \left[ \frac{v_{U_1} + v_{U_2}}{v} \right]$$

$$\frac{ig}{2} \rho_{\mu\nu} \left[ \frac{v_{U_1} + v_{U_2}}{v} \right]$$